



**Murdoch**  
UNIVERSITY

**MURDOCH RESEARCH REPOSITORY**

*This is the author's final version of the work, as accepted for publication following peer review but without the publisher's layout or pagination.*

*The definitive version is available at*

<http://dx.doi.org/10.1039/c5dt02129d>

**Königsberger, L.C., Königsberger, E., Hefter, G. and May, P.M.  
(2015) Formation constants of copper(i) complexes with  
cysteine, penicillamine and glutathione: implications for copper  
speciation in the human eye. Dalton Transactions, 44 (47).  
pp. 20413-20425.**

<http://researchrepository.murdoch.edu.au/29227/>

Copyright: © The Royal Society of Chemistry 2015

It is posted here for your personal use. No further distribution is permitted.

# Formation constants of copper(I) complexes with cysteine, penicillamine and glutathione: implications for copper speciation in the human eye

Lan-Chi Königsberger\*, Erich Königsberger, Glenn Hefter and Peter M. May

Chemical and Metallurgical Engineering and Chemistry, School of Engineering and Information Technology, Murdoch University, Murdoch WA6150, Australia.

E-mail:

L.Koenigsberger@murdoch.edu.au

E.Koenigsberger@murdoch.edu.au

G.Hefter@murdoch.edu.au

P.May@murdoch.edu.au

Fax number:

+61 8 9310 1711

## ABSTRACT

Protonation constants for the biologically-important thioamino acids cysteine (CSH), penicillamine (PSH) and glutathione (GSH), and the formation constants of their complexes with Cu(I), have been measured at 25 °C and an ionic strength of 1.00 mol dm<sup>-3</sup> (Na)Cl using glass electrode potentiometry. The first successful characterisation of binary Cu(I)–CSH and Cu(I)–GSH species over the whole pH range was achieved in this study by the addition of a second thioamino acid, which prevented the precipitation that normally occurs. Appropriate combinations of binary and ternary (mixed ligand) titration data were used to optimise the speciation models and formation constants for the binary species. The results obtained differ significantly from literature data with respect to the detection and quantification of protonated and polynuclear complexes. The present results are thought to be more reliable because of the exceptionally wide pH and concentration ranges employed, the excellent reproducibility of the data, the close agreement between the calculated and observed formation functions, and the low standard deviations and absence of numerical correlation in the constants. The present formation constants were incorporated into a large Cu speciation model which was used to predict, for the first time, metal-ligand equilibria in the biofluids of the human eye. This simulation provided an explanation for the precipitation of metallic copper in lens and cornea, which is known to occur as a consequence of Wilson's disease.

## KEYWORDS

Copper(I), cysteine, penicillamine, glutathione, protonation, complexation, speciation, aqueous humour, human eye.

## INTRODUCTION

The fundamental role of copper in human physiology, pathology and medicine has been stressed in numerous reviews.<sup>1-4</sup> As a redox-active trace element, copper, usually as Cu(I) or Cu(II), acts as a catalytic and structural cofactor in the chemistry of a wide range of biomolecules.<sup>4</sup> Although Cu(I) is unstable to disproportionation to Cu(II) and Cu(s) in simple aqueous solutions (without complexing agents), there is increasing evidence that it is the predominant oxidation state in many physiological settings. By way of example, Cu(I) has been identified in transport proteins and is known to play an important role in copper homeostasis,<sup>5</sup> the delivery of copper to mitochondria,<sup>6</sup> tumour cell metastasis and cancer chemotherapy<sup>3</sup>. Furthermore, Cu(I) can act as a scavenger for superoxide radicals in tissues<sup>7</sup> and some complexes of Cu(I) are effective anti-inflammatory agents<sup>8</sup>. As a  $d^{10}$  ion, Cu(I) forms strong complexes with many organic ligands,<sup>9</sup> at least in part because of its 'back bonding' capabilities. Being a 'soft' ion,<sup>10</sup> Cu(I) has a particular tendency to bind to sulfur-containing ligands.

Due to this critical role of copper in biological systems, reliable knowledge of the interactions between Cu(I) and key ligands of biological relevance is important for understanding and modelling the behaviour of such systems. While there are many possible ligands that warrant study, the thioamino acids (Fig. 1): (*R*)-2-amino-3-sulfhydrylpropanoic acid (L-cysteine, HS-CH<sub>2</sub>-CH(NH<sub>2</sub>)-COOH, 'CSH'), (*S*)-2-amino-3-methyl-3-sulfanylbutanoic acid (D-penicillamine, HS-C(CH<sub>3</sub>)<sub>2</sub>-CH(NH<sub>2</sub>)-COOH, 'PSH'); and  $\gamma$ -L-glutamyl-L-cysteinylglycine (glutathione, HOOC-CH(NH<sub>2</sub>)-(CH<sub>2</sub>)<sub>2</sub>-CO-NH-CH(CH<sub>2</sub>-SH)-CO-NH-CH<sub>2</sub>-COOH, 'GSH') are of particular significance. Cysteine, which occurs in blood plasma in the micromolar range,<sup>11</sup> is one of the most important metal-binding agents in biological fluids<sup>12</sup>. Glutathione is a tri-peptide that also occurs in blood plasma<sup>13</sup> at concentrations of several  $\mu\text{mol dm}^{-3}$  ( $\mu\text{M}$ , where M is introduced as an abbreviation for the concentration unit  $\text{mol dm}^{-3}$ ) but at much higher levels (1 to 6 mM) in cells<sup>14</sup>. Glutathione is involved in the transport of Cu(I) among proteins and enzymes<sup>15,16</sup> and in the way cells respond to heavy metal poisoning.<sup>17</sup> The drug penicillamine has been commonly employed as a treatment for Wilson's disease<sup>18,19</sup> and has also been widely used to treat rheumatoid arthritis<sup>20</sup>. Interestingly, the naturally-occurring thioamino acids cysteine and glutathione are conspicuously inactive as therapeutics.<sup>21</sup> Given all of these aspects it is of interest to have a more detailed knowledge of the interactions of Cu(I) with these ligands.

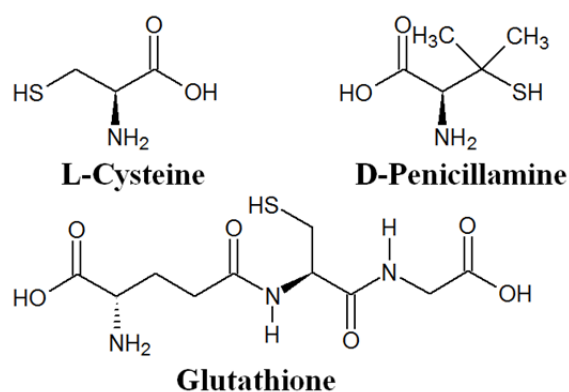


Fig. 1 Structural formulas of the thioamino acids CSH, PSH and GSH.

Unfortunately, quantification of Cu(I)–thioamino acid systems is not easy. The major reasons for this are: (i) Cu(I) is readily oxidised or, as noted above, disproportionates to Cu(II) in aqueous media in the absence of suitable complexing agents;<sup>22</sup> (ii) both the thioamino acids and their complexes are also readily oxidised; (iii) sparingly soluble precipitates are formed over wide pH ranges (especially with cysteine and glutathione); and (iv) all of these systems show pronounced tendencies to form protonated and polynuclear complexes.<sup>23</sup> In spite of these difficulties the biological relevance of the Cu(I) complexes of these particular thioamino acids has motivated many attempts to characterize them. Unfortunately, however, there is little agreement about the stoichiometry of the species formed, let alone their formation constants (see, *e.g.*, Refs. 24–26). In part this is because many of the previous studies were restricted to narrow ranges of conditions, mostly due to solubility limitations, with some measurements even being made at just a single pH.<sup>16,25,26</sup>

The development by Hefter *et al.*<sup>27</sup> of a reliable, generalized method for the quantitative study of Cu(I) complexes in aqueous solution, along with the availability of modern computational analysis, provides a basis for a thorough re-investigation of these systems. Accordingly, the present study reports the determination, by high-precision glass-electrode potentiometry, of the protonation constants of the thioamino acids CSH, PSH and GSH, and the formation constants of their complexes with Cu(I). Problems with precipitation were circumvented by the addition of a second thioamino acid, which produced solutions that remained homogeneous over the whole pH range.<sup>28</sup>

The formation constants measured were incorporated into the JESS reaction database<sup>29</sup> and used to calculate, for the first time, Cu speciation in the aqueous humour and lens fluid of the human eye. By taking into account the redox state of these fluids and tissues, the simulations provided an insight into the conditions for the precipitation of metallic copper which is known to be connected to the increased *in vivo* copper concentrations associated with Wilson's disease.

## EXPERIMENTAL AND COMPUTATIONAL METHODS

**Materials.** Analytical-grade reagents were used throughout. Concentrated volumetric standard solutions of HCl, NaOH, EDTA and CuCl<sub>2</sub> (BDH, UK) were employed where appropriate. Thioamino acids (Sigma-Aldrich, USA, ≥ 99 %), solid CuCl (Sigma-Aldrich, ≥ 99 %) and copper wire (99.99 %) were used as received. The ionic strength of all working solutions was kept constant at 1.00 M by the addition of NaCl (Ajax, Australia, 99.9 %). Concentrations of H<sup>+</sup> and OH<sup>-</sup> were cross-checked by acid-base titrations using Gran plots<sup>30</sup>. Alkali solutions were discarded after two weeks. All solutions were prepared using high purity water (Millipore Milli-Q system) that had been boiled and cooled under high purity (< 0.1 ppm O<sub>2</sub>) Ar to minimise dissolved O<sub>2</sub> and CO<sub>2</sub>.

**Apparatus.** Measurements were made with a computer-controlled high precision titration system incorporating a high-impedance digital voltmeter, Metrohm model 655 burettes fitted with anti-diffusion valves, and jacketed tall-form glass vessels (150 cm<sup>3</sup>) capped with tight-fitting machined PTFE tops. All measurements were made at 25.00 ± 0.01 °C. The galvanic cells used for the potentiometric titrations can be represented as:

Ag|AgCl | 5 M NaCl || 5 M NaCl || test solution,  $I = 1.00$  M (Na)Cl | GE

where GE is a glass electrode (Metrohm model 6.0101.000). Reference electrodes were either of commercial origin (Metrohm 6.0702.100) or 'homemade' using Ag wire in contact with solid AgCl and 5 M NaCl solution. Potentials were measured to 0.1 mV and stirring was provided by a PTFE-coated magnetic stirrer bar. Liquid junction potentials were assumed to be constant throughout. Glass electrodes were calibrated in terms of  $p[H]$  ( $= -\log_{10}[H^+]$ ) using a single point *in situ* procedure.<sup>31,32</sup> After calibration ( $dE/dt < 0.02$  mV/min) in a solution containing (10 to 50) mM HCl, thioamino acid and (where appropriate) Cu(I) solutions were added and the mixtures titrated with 0.1000 M NaOH. The Nernstian performance of the electrodes over the entire  $p[H]$  range was checked regularly by titrations of strong acid (HCl) against strong base (NaOH) solutions at  $I = 1.00$  M (Na)Cl.

**Copper(I) Generation.** The general method developed previously<sup>27</sup> for the determination of Cu(I) equilibria in aqueous solution was used. All operations were performed under high purity Ar. To minimise ingress of atmospheric gases, tubing was glass or copper, flexibly connected by the shortest possible lengths of PTFE bellows tubing. A stock solution of ~50 mM CuCl in 0.1 M HCl at  $I = 1.00$  M (Na)Cl was transferred to a 2 L round-bottomed flask containing a freshly cleaned (10 % HNO<sub>3</sub>) and dried Cu spiral and stirred for a few days under Ar. When required samples of this Cu(I) stock solution were withdrawn using a syringe burette. To ensure the integrity of the Cu(I) solution delivered to the titration cell, Cu spirals were also inserted into the connecting tubing and the burette cylinder. Three aliquots of the Cu(I) solution were withdrawn. The middle portion was used for titration while the first and last portions were analysed for  $[Cu(I)]_T$ , where the subscript T indicates the total or analytical concentration, by aerial oxidation to Cu(II) followed by titration against standard EDTA using fast sulfon black indicator<sup>33</sup>. Concentrations of  $H^+$  were determined from Gran plots of titrations with NaOH solution<sup>30</sup>. Stock solution concentrations were determined to  $\pm 0.1$  % and were found to drift only very slowly (*ca.* 1 % per month).

**Titration Procedure.** All solutions were maintained under high purity, pre-humidified Ar. Thioamino acid solutions were prepared immediately prior to titration with concentrations ranging from (5 to 21) mM for the protonation titrations. Metal + ligand titrations were performed with (4 to 10) mM total Cu(I) at metal/ligand ratios of 1:1, 2:3, 1:2, or 1:3 for the binary complexes and 1:1:1, 1:1:2, 1:1:3, 1:2:2 or 1:3:1 for the ternary (mixed ligand) systems; overall the ligand concentrations ranged between (4 to 25) mM. Precipitation, when present, typically occurred at  $2.3 \leq p[H] \leq 6.9$ ; under such circumstances, measurements commenced only after sufficient base had been added to dissolve any precipitates.

**Computational Analysis.** Potentiometric titration data were processed using the ESTA suite of programs.<sup>34-36</sup> Optimisations were carried out by a least squares minimisation of the objective function:

$$U = (N - n_p)^{-1} \sum_{n=1}^N n_e^{-1} \sum_{q=1}^{n_e} W_{nq} (Y_{nq}^{obs} - Y_{nq}^{calc})^2$$

where  $N$  is the total number of experimental titration points,  $n_p$  is the total number of parameters to be optimised,  $n_e$  is the total number of electrodes,  $Y_{nq}^{\text{obs}}$  and  $Y_{nq}^{\text{calc}}$  are the observed and calculated variable of the  $q^{\text{th}}$  residual at the  $n^{\text{th}}$  point respectively and  $W_{nq}$  is the corresponding weight at that point. Weights were calculated as:

$$W_{nq} = \left[ \sum_p \left( \frac{\delta(Y_{nq}^{\text{obs}} - Y_{nq}^{\text{calc}})}{\delta p} \right)^2 \sigma_p^2 \right]^{-1}$$

where  $p$  is the optimisation parameter and  $\sigma_p$  is the standard deviation of the titration parameters held constant during optimisation. Formation constants, electrode intercept  $E^{\circ'}$ , vessel and burette concentrations were optimised in various combinations. Both weighted and unweighted objective functions were used and the sum of squares of residuals was minimised with respect to both total concentrations (OBJT) and electrode potentials (OBJE). Since OBJT is less sensitive to errors near end points, it is preferred to OBJE, which would require the use of non-unit weights that are difficult to determine.<sup>35</sup> The electrode slope was assumed to be Nernstian (59.16 mV) throughout.

The simulation program ESTA1, which allows for the calculation of electrode potentials from titre volumes, formation constant estimation, species distributions and so on, was used to analyse the data, particularly to assess the goodness-of-fit.<sup>34-36</sup> A convenient graphical representation of the titration data is the proton formation function<sup>37</sup>,  $\bar{Z}_H$ , defined as:

$$\bar{Z}_H = \frac{T_H - [\text{H}^+] + [\text{OH}^-]}{T_L}$$

where  $T_L$  is the total ligand concentration,  $[\text{OH}^-] = K_w/[\text{H}^+]$  and  $K_w$  is the ionic product of water under the titration conditions. The corresponding metal formation function<sup>37</sup>,  $\bar{Z}_M$ , is:

$$\bar{Z}_M = \frac{T_L - A \left( 1 + \sum_n \beta_{\text{LH}_n} [\text{H}^+]^n \right)}{T_M}$$

where  $T_M$  is the total metal concentration and

$$A = \frac{T_H - [\text{H}^+] + [\text{OH}^-]}{\sum_n n \beta_{\text{LH}_n} [\text{H}^+]^n}$$

For ternary systems,  $\bar{Z}_H$  is defined with  $T_L = T_{L1} + T_{L2}$  but  $\bar{Z}_M$  is undefined.

For the protonation constants, a Monte Carlo analysis was performed with 75 cycles to identify the parameters best refined simultaneously with the formation constants, the chosen set being the one that gave the smallest standard deviation in the parameters of interest. Full details of this procedure are given elsewhere.<sup>36</sup> In contrast, metal-ligand formation constants were optimised without other parameters. Model selection was based on the magnitudes of the objective functions, the standard deviations of the constants, and graphical comparison of the observed and calculated  $\bar{Z}_H$  and  $\bar{Z}_M$  curves. Because of their more distinctive separation for titrations with different metal-to-ligand ratios,  $\bar{Z}_H$  plots are shown for all systems. These

plots illustrate the reproducibility of the titrations and the good fit between the experimental and calculated data. For illustrative purposes, a plot of  $\bar{Z}_M$  for the Cu(I)–CSH system is shown in the ESI (Fig. S4). However, it should be noted: (i)  $\bar{Z}_M$  curves for this system cannot be interpreted in a simple way and (ii) to distinguish clearly between multiple curves, fewer titrations have been plotted than in the  $\bar{Z}_H$  plot (Fig. 4) for the same system.

Overall formation constants,  $\beta_{pqsr}$ , corresponding to the equilibrium (ignoring charges):



with

$$\beta_{pqsr} = [M'_pL_qL'_sH_r] / [M']^p [L]^q [L']^s [H]^r$$

where  $M'$  is Cu(I),  $L$  is the thioamino acid ligand,  $L'$  is a second thioamino acid ligand (if present), and  $H$  is  $H^+$ , were employed throughout.

## RESULTS AND DISCUSSION

### Protonation Constants

**General Comments.** The experimental data used to determine the protonation constants of CSH, PSH and GSH are summarized in Table S1 in the Electronic Supplementary Information (ESI). The constants obtained are given in Table 1 together with their standard deviations calculated from the Monte Carlo analyses using an unweighted OBJT function. Note that such deviations were generated from the computational analysis; real errors can be up to an order of magnitude larger.<sup>38</sup> The small objective functions are indicative of the reproducibility of the titration data and the goodness-of-fit of the models. The quality of the present results is further illustrated by the  $\bar{Z}_H$  plot in Fig. 2, which includes all the data obtained from 18 titrations with solutions ranging from (5 to 21) mM GSH. The individual data sets and the model are virtually indistinguishable. The even more reproducible results obtained for the more stable CSH and PSH are shown in Figs. S1 and S2 in the ESI.

Table 1 Measured protonation constants of the thioamino acids CSH, PSH and GSH at 25 °C in  $I = 1.00$  M (Na)Cl.

Systems	OBJT	$\lg\beta_{011} \pm \sigma$	$\lg\beta_{012} \pm \sigma$	$\lg\beta_{013} \pm \sigma$	$\lg\beta_{014} \pm \sigma$
CSH	5.29E–9	10.164 ± 0.006	18.36 ± 0.01	20.34 ± 0.02	
PSH	4.88E–9	10.470 ± 0.006	18.46 ± 0.01	20.48 ± 0.01	
GSH	1.08E–8	9.357 ± 0.004	17.970 ± 0.007	21.40 ± 0.01	23.60 ± 0.01

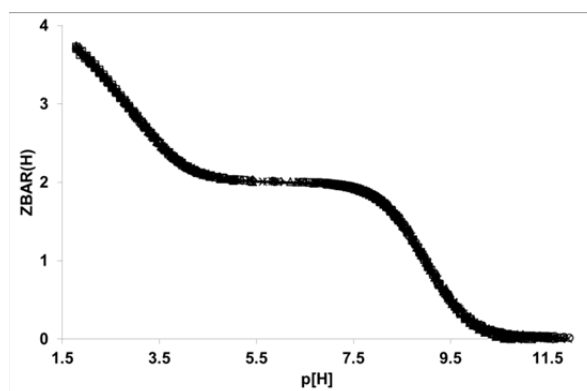


Fig. 2 Proton formation function for GSH at 25 °C and  $I = 1.00$  M (Na)Cl. Open symbols, experimental data; solid line, calculated curve.

**Cysteine.** The present protonation constants for CSH are compared with literature values obtained at  $I = 1$  M in various media in Table 2. Agreement amongst these studies is good, with the near-quantitative agreement between the present results and the only other study in NaCl media<sup>39</sup> being particularly noteworthy.

Table 2 Comparison of the present and literature protonation constants for CSH at 25 °C and  $I = 1$  M in various media.

Medium	$\lg\beta_{011}$	$\lg\beta_{012}$	$\lg\beta_{013}$	Reference
NaCl	10.164	18.36	20.34	This work
NaCl	10.193	18.372	20.271	39
NaClO <sub>4</sub>	10.19	18.44	20.53	40
NaNO <sub>3</sub>	10.15	18.27	20.17	41

**Penicillamine.** To the best of our knowledge, no protonation constants for PSH have been reported in the literature at  $I = 1$  M in any medium. However the present results (Table 1) are in good agreement with the values  $\lg\beta_{011} = 10.50$ ,  $\lg\beta_{012} = 18.42$  and  $\lg\beta_{013} = 20.37$  reported at 25 °C and  $I = 0.5$  M NaClO<sub>4</sub> by Österberg *et al.*<sup>14</sup> The reliability of the present constants is supported by the reproducibility of the data and the good fit between the observed and calculated  $\bar{Z}_H$  curves (Fig. S2 in the ESI). Fig. 1 shows that PSH has similar structure to CSH but has two methyl groups on the  $\alpha$ -carbon atom adjacent to the thiol group. This decreases the acidity of PSH relative to CSH,<sup>42</sup> consistent with their protonation constants (Table 1).

**Glutathione.** Table 3 compares the present protonation constants for GSH with literature values obtained at  $I = 1$  M in various media (there are a multitude of values reported for other conditions<sup>17</sup>). Although GSH is the most difficult of the present systems to quantify, being the most easily oxidized and having the most ionisable protons, the agreement among the various studies is very good, except for the early work of Stricks and Kolthoff.<sup>44</sup> The



agreement between the present results and those of Crea *et al.*<sup>17</sup> obtained under almost identical conditions in NaCl and in 1.0 M (KCl) is particularly gratifying.

Table 3 Comparison of the present and literature protonation constants for GSH at 25 °C and  $I = 1$  M in various media.

Medium	$\lg\beta_{011}$	$\lg\beta_{012}$	$\lg\beta_{013}$	$\lg\beta_{014}$	Reference
NaCl	9.357	17.970	21.40	23.60	Present work
NaCl <sup>a</sup>	9.302	17.884	21.375	23.616	17
KCl	9.38	17.96	21.42	23.68	17
KNO <sub>3</sub>	9.69	18.44	21.93	23.91	43
KNO <sub>3</sub>	8.82	17.78			44

<sup>a</sup> At  $I = 0.93$  M (NaCl); similar values were also reported at  $I = 1.4$  M (NaCl).<sup>17</sup>

## Cu(I)–Thioamino Acid Systems

**General Comments.** Before discussing the individual Cu(I)–thioamino acid systems, a few general comments on their quantification are appropriate. The present experimental approach was designed to ensure that all dissolved copper was present as Cu(I), stabilized by excess Cl<sup>−</sup> and/or any thioamino acids present. In addition, independently prepared Cu(I) stock solutions, freshly prepared ligand solutions of varying concentration, and differing Cu(I):ligand ratios were used throughout. The titration data obtained in this manner are summarised in Table S2 in the ESI.

It is important to recognize that measurements on the binary Cu(I)–CSH and Cu(I)–GSH systems were severely restricted by precipitation over a wide range of p[H] ( $< 5.2$  and  $2.3 < p[H] < 6.9$ , respectively). Fortunately, it was found that the addition of a second thioamino acid suppressed the precipitation such that satisfactory data could be obtained over the whole p[H] range of interest.<sup>28</sup> To the best of our knowledge this is the first time that this has been achieved: previous studies have mostly been measured over very restricted concentration ranges, sometimes at only one pH.<sup>25,26</sup> The availability of reliable data for the *ternary* (mixed ligand) systems<sup>28</sup> allowed the formation constants of the *binary* Cu(I)–CSH and Cu(I)–GSH systems to be refined in a manner that was impossible using the (truncated) binary data alone.

Another significant problem in the quantification of Cu(I)–thioamino acid systems is their tendency to form protonated and polynuclear complexes. This complicates model selection and makes imperative the availability of high quality data over wide concentration ranges of Cu(I), ligand and proton. The challenges in studying these systems are reflected in the lack of agreement among independent researchers, stretching over many decades, on the stoichiometry of the species formed, let alone the magnitudes of their corresponding formation constants.

**Cu(I)–PSH Complexes.** Among the three Cu(I)–thioamino acid systems studied, Cu(I)–PSH was the least complicated because there was no precipitation and titration data could be collected over a wide p[H] range ( $1.7 \leq p[H] \leq 11.5$ ). The data obtained were best

modelled with the species  $\text{Cu}(\text{PS})^-$ ,  $\text{Cu}(\text{PS})\text{H}^0$ ,  $\text{Cu}_2(\text{PS})_2\text{H}^-$  and  $\text{Cu}_2(\text{PS})\text{H}^+$  (Table 4). The reproducibility of the data and the agreement between the calculated and observed  $\bar{Z}_H$  curves are shown in Fig. S3 in the ESI.

Also included in Table 4 are literature values of the formation constants for the Cu(I)–PSH system obtained under conditions broadly similar to the present work. The presence of  $\text{Cu}(\text{PS})^-$  has been claimed in several studies<sup>45,46</sup> but there are large differences in the reported formation constants. The present result ( $\lg\beta_{110} = 12.42$ ) is about the average of the earlier values, although it should be noted that the work of Vortisch *et al.*<sup>45</sup> is not strictly comparable with the present study as their measurements were made in aqueous acetonitrile solutions.

The species distribution for the Cu(I)–PSH system is shown as a function of p[H] at two Cu(I):PSH ratios in Fig. 3. The most notable features of the distribution diagram were the dominance of dinuclear and/or protonated species ( $\text{Cu}_2(\text{PS})\text{H}^+$ ,  $\text{Cu}(\text{PS})\text{H}^0$  and  $\text{Cu}_2(\text{PS})_2\text{H}^-$ ) regardless of the Cu(I):PSH ratio. The simplest mononuclear species,  $\text{Cu}(\text{PS})^-$ , only became dominant at p[H] > ca. 7.5. Significant amounts of free Cu(I) existed at p[H] < 2 at all Cu(I):PSH ratios but became negligible at p[H] > 6 (Fig. 3).

There is broad agreement amongst the various studies of the Cu(I)–PSH system in that polynuclear complexes have been detected, although rather few have been quantified (Table 4). Marked differences between the present and previous investigations exist with regard to the detection of protonated complexes. For example, Vortisch *et al.*<sup>45</sup> reported  $\text{Cu}_2(\text{PS})^0$  whereas the protonated form,  $\text{Cu}_2(\text{PS})\text{H}^+$ , was detected in the present study. In a similar vein,  $\text{Cu}_2(\text{PS})_3^{4-}$  was reported in several studies,<sup>25,45,46</sup> while  $\text{Cu}_2(\text{PS})_2\text{H}^-$  was identified in this work. The most likely explanation for these differences is that the present study covers a much wider p[H] range. For example, Mezyk and Armstrong<sup>25</sup> reported  $\text{Cu}_2(\text{PS})_3^{4-}$  and  $\text{Cu}(\text{PS})_2^{3-}$  from UV spectra recorded only at p[H] = 10.0; protonated species are negligible at this p[H] (Fig. 3). The species  $\text{Cu}(\text{PS})_2^{3-}$ , claimed in Refs. 25 and 46, was not detected in Ref. 45 or in the present study. Österberg *et al.*<sup>14</sup> reported only  $\text{Cu}(\text{PS})_2\text{H}_2^-$  and  $\text{Cu}_5(\text{PS})_4^{3-}$  but no evidence could be found in the present work for any of these species despite extensive modelling.

Table 4 Present and literature values for the formation constants of Cu(I)–PSH complexes.

Method <sup>a</sup>	t/°C	Medium/M	lgβ(σ)	Reference
Poty	25	1 (NaCl)	$\beta_{110}$ 12.42(6); $\beta_{111}$ 18.72(4); $\beta_{211}$ 22.29(9); $\beta_{221}$ 34.44(10)	Present work <sup>b</sup>
Poty	25	0.5 (NaClO <sub>4</sub> )	$\beta_{122}$ 39.18(3); $\beta_{540}$ 101.50(5)	14
Spec	23	0.05 <sup>c</sup>	$\beta_{120}^d$ ; $\beta_{230}^{d,e}$	25
Poty	20	0.1 (NaClO <sub>4</sub> ) <sup>f</sup>	$\beta_{110}$ 14.3; $\beta_{210}^d$ ; $\beta_{230}^d$	45
Spec	20	1 (NaClO <sub>4</sub> )	$\beta_{110}$ 10.52; $\beta_{120}^d$ ; $\beta_{230}^d$	46

<sup>a</sup> Abbreviations: Poty – glass electrode potentiometry; Spec – UV-vis spectrophotometry. <sup>b</sup> OBJT = 1.02E–8. <sup>c</sup> Measured at pH = 10.0 only. <sup>d</sup> Complex detected but no value given for the formation constant. <sup>e</sup>  $\lg K = 113(14)$  was also reported for the equilibrium:  $2 \text{Cu}(\text{PS})_2^{3-} \rightleftharpoons \text{Cu}_2(\text{PS})_3^{4-} + (\text{PS})^{2-}$ . <sup>f</sup> In 1 M CH<sub>3</sub>CN.

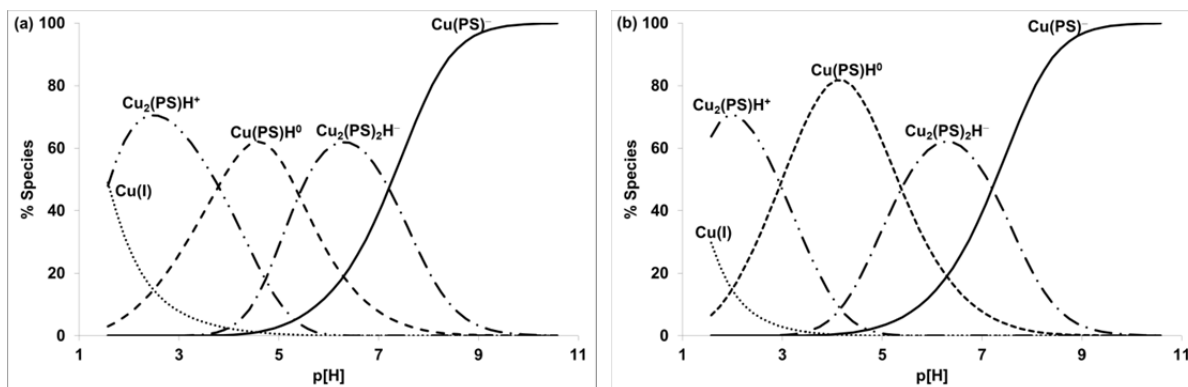


Fig. 3 Species distribution of Cu(I)–PSH with  $[Cu]_T = 5$  mM at: (a) Cu:PSH = 1:1 and (b) Cu:PSH = 1:3. Dotted line: free Cu(I); dash-dot-dot:  $Cu_2(PS)H^+$ ; dash-dash:  $Cu(PS)H^0$ ; dash-dot:  $Cu_2(PS)_2H^-$  and solid curve:  $Cu(PS)^-$ .

**Cu(I)–CSH Complexes.** The accessible p[H] region in the binary Cu(I)–CSH system was restricted to  $p[H] > 5.2$  due to precipitation (Fig. 4). Insufficient experimental information resulted in correlated formation constants which precluded determination of  $\lg\beta_{110}$ . Most studies of this system agree on the existence of  $Cu(CS)^-$  but the reported  $\beta_{110}$  values vary by almost eight orders of magnitude (Table 5). This sort of disagreement among independent studies usually indicates that the system is inherently complicated: either because of the number of overlapping species and/or the presence of specific experimental problems.<sup>36,37,47</sup> Regardless, a value of  $\beta_{110}$  is required to achieve convergence and to fix the numerical values of the other formation constants, even though the value chosen has little effect on the stepwise formation constants of subsequent species. The value selected,  $\lg\beta_{110} = 13.13$ , was determined polarographically at the same ionic strength and temperature in this laboratory<sup>48</sup> and is the approximate average of the  $\lg\beta_{110}$  values reported by Vortisch *et al.*<sup>45</sup> and Bagiyani *et al.*<sup>46</sup>.

Using this value along with the binary Cu(I)–CSH data in the homogeneous region ( $5.2 \leq p[H] \leq 11.4$ ) yielded a model comprising  $Cu(CS)^-$ ,  $Cu_2(CS)_3H_3^-$ ,  $Cu_2(CS)_2H^-$  and  $Cu_2(CS)^0$  that accurately represented the experimental observations over this restricted p[H] range (Fig. 4 and Fig. S4 in the ESI). The addition of PSH to the Cu(I)–CSH system permitted data to be obtained without precipitation in the range  $1.5 \leq p[H] \leq 11.9$  (Fig. S5, Tables S3 and S4 in the ESI). The inclusion of  $Cu_2(CS)H^+$  in the ternary model lowered OBJT by more than an order of magnitude. The species distribution for the ternary system at Cu(I):CSH:PSH = 1:1:3 shows that the binary species  $Cu_2(CS)H^+$  is predominant at  $p[H] < 2.5$ .<sup>28</sup> The formation constants of the refined model for the Cu(I)–CSH binary system are given in Table 5. The corresponding species distribution is shown in Fig. 5. Where comparisons are possible (Tables 4 and 5) the Cu(I)–CSH complexes are  $\sim 3$  orders of magnitude stronger than Cu(I)–PSH, which is reflected in the absence of significant free Cu(I) concentrations over the entire p[H] range. Even at low p[H] the speciation is dominated by the dinuclear species  $Cu_2(CS)H^+$  and  $Cu_2(CS)^0$ . At  $p[H] > ca. 6$ ,  $Cu_2(CS)_3H_3^-$  becomes the predominant species especially, as would be expected, at higher Cu(I):CSH ratios. As for the Cu(I)–PSH system (Fig. 3), the simplest mononuclear complex,  $Cu(CS)^-$ , only becomes important at relatively high p[H] values (Fig. 5).

Also listed in Table 5 are the formation constants reported for the Cu(I)–CSH complexes in the literature under broadly comparable conditions to the present work. As for Cu(I)–PSH, there is little agreement among these studies as to the stoichiometry of the species formed and again a number of species have been identified but not quantified. Also as for Cu(I)–PSH, the major difference between the present results and previous investigations is the detection of protonated species. The tendency of CSH to form protonated and polynuclear complexes with a variety of metal ions is well known.<sup>23</sup> Interestingly, Bagiyan *et al.*<sup>46</sup> indicated that protonated complexes of  $\text{Cu}(\text{CS})^-$  formed readily during their pH-metric titrations but only reported a value for  $\beta_{110}$  (Table 5).

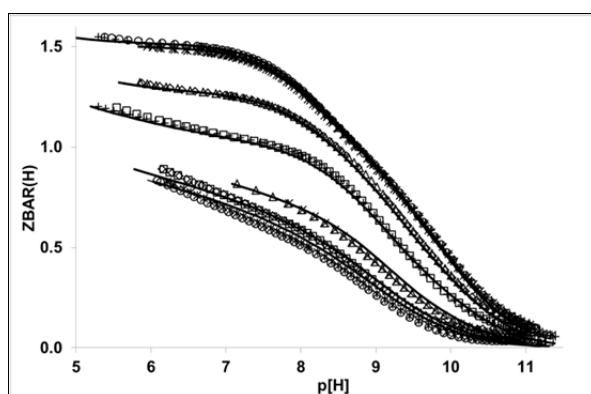


Fig. 4 Proton formation functions for Cu(I)–CSH at 25 °C and  $I = 1.00$  M (Na)Cl with  $[\text{Cu}(\text{I})]_{\text{T}} = (4 \text{ to } 5)$  mM. Open symbols, experimental data at Cu(I):CSH = 1:1, 2:3, 1:2 and 1:3; solid lines, calculated curves.

Table 5 Present and literature values for the formation constants of Cu(I)–CSH complexes.

Method <sup>a</sup>	$t/^\circ\text{C}$	Medium/M	$\lg\beta(\sigma)$	Reference
Poty	25	1 (NaCl)	$\beta_{110}$ 13.13 <sup>c</sup> ; $\beta_{210}$ 22.75(2); $\beta_{211}$ 25.36 <sup>d</sup> ; $\beta_{221}$ 37.65(5); $\beta_{233}$ 59.69(5)	This work <sup>b</sup>
Poly	25	1 (NH <sub>4</sub> Cl)	$\beta_{110}$ 19.19; $\beta_{210}$ <sup>e</sup>	24
Spec	23	0.05 <sup>f</sup>	$\beta_{120}$ <sup>e</sup> ; $\beta_{230}$ <sup>e,g</sup>	25
Fluoro	25	Buffers <sup>h</sup>	$\beta_{111}$ 23.0(1.4); $\beta_{122}$ 38.4(7.8)	26
Poty	20	0.1 (NaClO <sub>4</sub> )	$\beta_{110}$ 14.0; $\beta_{210}$ <sup>e</sup> ; $\beta_{230}$ <sup>e</sup>	45
Spec	20	1 (NaClO <sub>4</sub> )	$\beta_{110}$ 11.38; $\beta_{120}$ <sup>e</sup> ; $\beta_{230}$ <sup>e</sup>	46

<sup>a</sup> Abbreviations: Poty – glass electrode potentiometry; Poly – polarography; Spec – UV-vis spectrophotometry; Fluoro – fluorometric titrations. <sup>b</sup> OBJT = 1.07E–8. <sup>c</sup> Determined by polarography<sup>48</sup>. <sup>d</sup> Determined from the ternary Cu(I)–CSH–PSH potentiometric titrations<sup>28</sup>. <sup>e</sup> Complex detected but no value given for the formation constant. <sup>f</sup> Measured at pH = 10.0 only. <sup>g</sup>  $\lg K = 162(23)$  reported for the equilibrium:  $2 \text{Cu}(\text{CS})_2^{3-} \rightleftharpoons \text{Cu}_2(\text{CS})_3^{4-} + (\text{CS})^{2-}$ . <sup>h</sup> Determined in buffer solutions at pH = 7.2, 8.1 and 9.0.

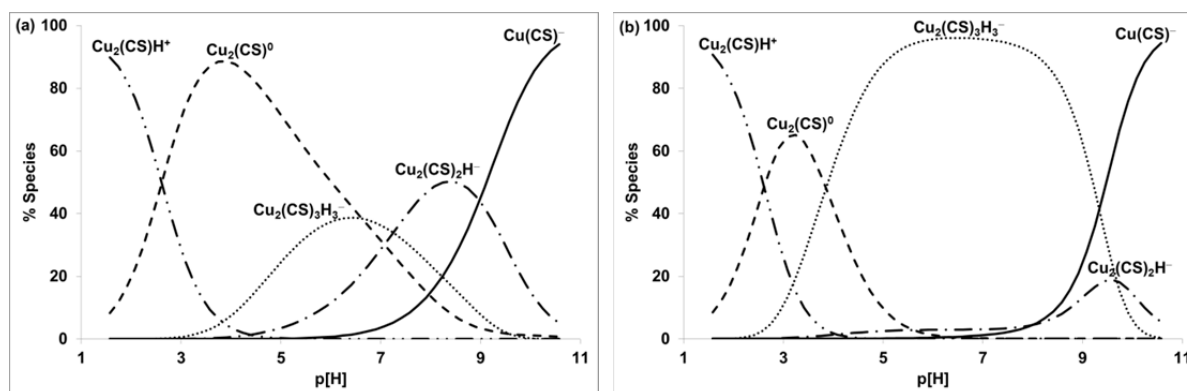


Fig. 5 Species distribution of Cu(I)–CSH with  $[Cu]_T = 5 \text{ mM}$  at (a) Cu:CSH = 1:1 and (b) Cu:CSH = 1:3. Dash-dot-dot:  $Cu_2(CS)H^+$ ; dash-dash:  $Cu_2(CS)^0$ ; dotted line:  $Cu_2(CS)_3H_3^-$ ; dash-dot:  $Cu_2(CS)_2H^-$  and solid curve:  $Cu(CS)^-$ . Since precipitation occurs in the binary system, curves are hypothetical at  $p[H] < 5.2$ . Consequently, the formation constant for  $Cu_2(CS)H^+$  was determined from the ternary Cu(I)–CSH–PSH potentiometric titrations.<sup>28</sup>

Consistent with the present findings, Harman and S3v3g3o<sup>49</sup> have pointed out that the degree of formation and stoichiometry of  $M^{n+}$ –PSH polynuclear complexes should be markedly different from those for  $M^{n+}$ –CSH due to steric inhibition by the  $\beta$ -methyl substituents in the former. This insight contrasts markedly with earlier investigations<sup>25,45,46</sup> that assumed the same model for Cu(I)–CSH and Cu(I)–PSH.

**Cu(I)–GSH Complexes.** Precipitation is more severe in the Cu(I)–GSH binary system than in Cu(I)–CSH, occurring over the range  $2.3 < p[H] < 6.9$  (Fig. S6 in the ESI). Using the binary system data, the ‘best’ model consisting of  $Cu(GS)^{2-}$ ,  $Cu(GS)H^-$ ,  $Cu(GS)H_3^+$ ,  $Cu(GS)_2H^{4-}$ ,  $Cu(GS)_2H_2^{3-}$  converged, but with correlated formation constants. The addition of a second ligand, CSH, enabled data to be collected at  $1.4 \leq p[H] \leq 11.6$  (Fig. S7, Tables S3 and S4 in the ESI) from which the formation constants for  $Cu(GS)H_3^+$  and  $Cu(GS)H^-$  could be unambiguously evaluated. In the species distribution for the ternary system at Cu(I):CSH:GSH = 1:1:1, these binary species contribute up to 40 % of total Cu at  $p[H]$  of 1.5 and 4.5 respectively.<sup>28</sup> Furthermore, with the refined formation constants of these two species, a re-investigation of the binary model showed that the introduction of  $Cu_2(GS)H^0$  improved OBJT and the standard deviation of the binary species in the model. The formation constants for the binary complexes:  $Cu(GS)^{2-}$ ,  $Cu(GS)H^-$ ,  $Cu(GS)H_3^+$ ,  $Cu(GS)_2H^{4-}$ ,  $Cu(GS)_2H_2^{3-}$  and  $Cu_2(GS)H^0$  are listed in Table 6 and species distribution curves are shown in Fig. 6.

While more species were detected in this system than for Cu(I)–PSH and Cu(I)–CSH (compare Tables 4, 5 & 6) the speciation is dominated at  $3 \leq p[H] \leq 9$  by a single species,  $Cu(GS)H^-$ . The relative concentrations of the various species are more sensitive to the Cu(I):ligand ratio than the other systems (compare Figs. 3, 5 & 6). Another significant difference between Cu(I)–GSH and the other two systems is that most of the detected species are mononuclear. On the other hand, as for the other systems, the simplest (110) species,  $Cu(GS)^{2-}$ , is formed significantly only at high  $p[H]$ . The only polynuclear species observed in

this system is the neutral complex,  $\text{Cu}_2(\text{GS})\text{H}^0$ , which predominates only over a narrow  $\text{p}[\text{H}]$  range (Fig. 6).

Comparison of the present results with selected literature data (Table 6) again shows little agreement although, consistent with the present findings, both  $\text{Cu}(\text{GS})_2\text{H}_2^{3-}$  and the dominant  $\text{Cu}(\text{GS})\text{H}^-$  were detected and quantified by other investigators.<sup>14,26</sup>

Table 6 Present and literature values for the formation constants of Cu(I)–GSH complexes at 25 °C.

Method <sup>a</sup>	Medium/M	$\lg\beta(\sigma)$	Reference
Poty	1 (NaCl)	$\beta_{110}$ 11.05(3); $\beta_{111}$ 20.27 <sup>c</sup> ; $\beta_{113}$ 26.04 <sup>c</sup> ; $\beta_{121}$ 23.24(2); $\beta_{122}$ 32.63(3); $\beta_{211}$ 24.89(10)	This work <sup>b</sup>
Poty	0.5 (NaClO <sub>4</sub> )	$\beta_{111}$ 24.9; $\beta_{122}$ 38.8(1)	14
Fluoro	Buffers <sup>d</sup>	$\beta_{111}$ 22.3(6); $\beta_{122}$ 35.5(1.1)	26

<sup>a</sup> Abbreviations: Poty – glass electrode potentiometry; Fluoro – fluorometric titrations.

<sup>b</sup> OBJT = 4.39E–8. <sup>c</sup> Determined from the ternary Cu(I)–CSH–GSH potentiometric titrations<sup>28</sup>. <sup>d</sup> Determined in buffer solutions at  $\text{pH} = 7.2, 8.1$  and  $9.0$ .

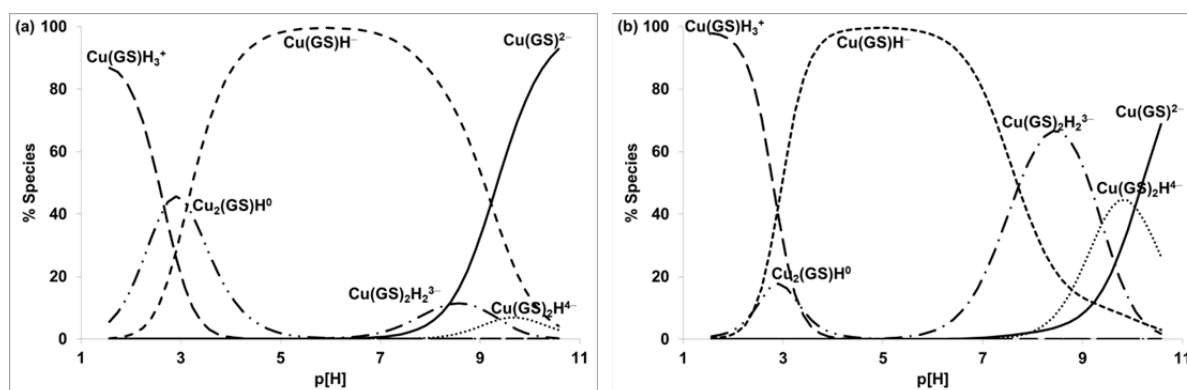


Fig. 6 Species distribution of Cu(I)–GSH from the refined model with  $[\text{Cu}]_{\text{T}} = 5 \text{ mM}$  at (a)  $\text{Cu}:\text{GSH} = 1:1$  and (b)  $\text{Cu}:\text{GSH} = 1:3$ . Long dash:  $\text{Cu}(\text{GS})\text{H}_3^+$ ; dash-dot-dot:  $\text{Cu}_2(\text{GS})\text{H}^0$ ; short dash:  $\text{Cu}(\text{GS})\text{H}^-$ ; dash-dot:  $\text{Cu}(\text{GS})_2\text{H}_2^{3-}$ ; dotted line:  $\text{Cu}(\text{GS})_2\text{H}^{4-}$  and solid curve:  $\text{Cu}(\text{GS})_2^{2-}$ . Since precipitation occurs in the binary system, curves are hypothetical in the range  $2.3 < \text{p}[\text{H}] < 6.9$ . Consequently, the formation constant for  $\text{Cu}(\text{GS})\text{H}_3^+$  and  $\text{Cu}(\text{GS})\text{H}^-$  were refined from the ternary Cu(I)–CSH–GSH potentiometric titrations.<sup>28</sup>

Of particular interest are studies that provide direct structural information for Cu(I)–GSH species. Corazzo *et al.*<sup>15</sup> have applied <sup>1</sup>H-NMR, <sup>13</sup>C-NMR and X-ray absorption spectroscopy to Cu(I)–GSH solutions of varying  $\text{pH}$  and  $\text{GSH}:\text{Cu}(\text{I})$ . From <sup>1</sup>H-NMR spectra of GSH as a function of  $\text{pH}$ , they derived microscopic protonation constants which show some parallels with the macroscopic constants obtained in this work (Table 3). Their <sup>1</sup>H-NMR data for Cu(I)–GSH solutions indicated deprotonation steps at  $\text{pH} \approx 10$ , which are compatible with the deprotonation of the  $\text{Cu}(\text{GS})\text{H}^-$  and  $\text{Cu}(\text{GS})_2\text{H}_2^{3-}$  species around this  $\text{pH}$  observed in the

present work (Fig. 6). Also from  $^1\text{H-NMR}$  data, Corazzo *et al.*<sup>15</sup> derived a GSH:Cu(I) ratio of *ca.* 1.2 in the Cu(I)–GSH species present at pH = 7.2. This is again in accordance with Fig. 6 which shows a mixture of predominantly  $\text{Cu}(\text{GS})\text{H}^-$  and a small amount of  $\text{Cu}(\text{GS})_2\text{H}_2^{3-}$  at this pH. However, these parallels might just be fortuitous given that Corazzo *et al.*<sup>15</sup> used phosphate buffers in  $\text{D}_2\text{O}$  (without applying corrections to pH meter readings), up to 10 times greater GSH and much lower  $\text{Cl}^-$  concentrations than those employed in the present study.

Both Corazzo *et al.*<sup>15</sup> and Poger *et al.*<sup>16</sup> performed X-ray absorption measurements (mostly at just one GSH concentration, one or two GSH:Cu(I) ratios, one pH and low or zero  $\text{Cl}^-$  concentration) and concluded that Cu(I) is coordinated by 3 sulfur atoms. To account for measured GSH:Cu(I) ratios of 1.2<sup>15</sup> and 2.5<sup>16</sup> in the Cu(I)–GSH complexes, they proposed polymeric<sup>15</sup> and a dinuclear species,  $\text{Cu}_2(\text{GS})_5$ ,<sup>16</sup> respectively. Such species were not detected in the present study, although GSH:Cu(I) ratios ranging from 1:1 to 3:1 were investigated. The Cu(I)–GSH species containing fewer GSH ligands found in the present study appear plausible because Cu(I) is expected to be significantly coordinated to  $\text{Cl}^-$  at 1 M NaCl. However, Corazzo *et al.*<sup>15</sup> investigated solutions without and with  $\text{Cl}^-$  (albeit at much lower concentration resulting from  $\text{CuCl}(\text{s})$  used for sample preparation) and concluded that  $\text{Cl}^-$  can be discounted as a ligand for Cu(I). We therefore cannot explain the differences between our findings and those reported by them. However, under biological conditions when the total Cu(I) concentration is in the  $\mu\text{M}$  range (see below) and the free Cu(I) is estimated to be very much less (say  $\sim 1$  pM) so that dimeric or polymeric Cu(I) species are most unlikely to predominate.

Since GSH:Cu(I) ratios can change by several orders of magnitude in different biological contexts and almost no techniques are available to study metal-ligand binding directly at biological concentrations, neither the present potentiometric titrations nor the spectroscopic studies discussed above<sup>15,16</sup> can unequivocally determine the ‘true’ Cu(I)–GSH speciation under biological conditions. However, speciation modelling represents a viable way forward to extrapolate, in a thermodynamically rigorous way, to concentrations far below those which can be investigated experimentally.<sup>29</sup> The physiological relevance of speciation models based on the present data is evidenced by the fact that they provide the first explanation of the formation of Kayser-Fleischer rings in the human eye from precipitation of metallic copper.

## Thermodynamic Modelling of Copper Speciation in the Human Eye

The aqueous humour (‘AH’) of the human eye is enclosed in the small anterior (250  $\mu\text{L}$ ) and posterior (60  $\mu\text{L}$ ) chambers of the eye, the space between the lens and the cornea. It is a transparent, gelatinous fluid similar to blood plasma (‘BP’) but with a marked deficit of protein (0.02 % *vs.* 7 % in BP) and a 15 times higher concentration of ascorbate. The concentrations of trace metals like Cu and Fe, and of antioxidants such as ascorbate, glutathione and cysteine in the AH have been investigated extensively because they serve as markers for diseases and infections of the eye. Compared to healthy subjects, patients suffering from glaucoma, cataracts or diabetes generally have elevated copper concentrations in the lens and the vitreous and aqueous humours<sup>50</sup>. In Wilson’s disease (‘WD’), a rare genetic disorder that inhibits Cu excretion in the bile, Cu concentrations can become so high that metallic copper is precipitated in the cornea or the lens, giving rise to so-called ‘Kayser-Fleischer rings’<sup>51</sup> or ‘sunflower cataracts’<sup>52</sup> respectively. These ocular manifestations of WD generally disappear following treatment with Cu-chelating agents, such as D-penicillamine.

The circulation of AH supplies nutrients and removes metabolites from the avascular cornea and lens. The oxygen concentration in the anterior AH, which is partly maintained by direct diffusion of O<sub>2</sub>(g) through the cornea, is higher than in arterial blood.<sup>53</sup> Such O<sub>2</sub> levels, in combination with UV radiation, require efficient mechanisms for the removal of highly reactive oxygen species ('ROS') that can cause tissue damage. Ascorbic acid and (reduced) thioamino acids are thus important low-molecular-weight antioxidants that keep the redox state of the AH at negative (reducing) values.

In this work the Joint Expert Speciation System, JESS<sup>29</sup>, has been used to estimate the redox state and the speciation of copper in the AH of the human eye. Our previous simulations of copper speciation among low-molecular-weight ligands in blood plasma<sup>28,29</sup> have established the prevalence of Cu(I) complexes with cysteine and glutathione. For the present calculations, six metals (including the redox-active trace metals Cu and Fe), some 40 ligands, a total of almost 5000 species and more than 5300 reactions were included in the model. Accurate formation constants for the Cu(I)–thioamino acid complexes, obtained in the present work, underpinned these calculations. As for the BP models,<sup>28,29</sup> the conditions for the present JESS simulations were chosen to be: a temperature of 25 °C and an ionic strength of 0.15 M, since most of the relevant complex formation constants have been reported for these conditions. While these conditions are not optimal, previous experience<sup>28,29</sup> indicates that it is generally advisable to base modelling calculations on the best-characterised data and to adjust the parameters to match other conditions using appropriate thermodynamic relationships. In this study, the formation constants were determined in 1 M NaCl and were adjusted to the desired ionic strength of 0.15 M using a modified SIT equation.<sup>54</sup>

**Concentrations of redox-active ligands and redox state.** The delicate interplay between various thiol/disulfide redox systems and ROSs in both redox signalling and oxidative stress has been reviewed recently.<sup>55</sup> Owing to significant variations in the concentrations of reduced and oxidised species in the glutathione and cysteine pools of plasma, cytoplasm, nucleus and other organelles, the redox potentials as calculated by the Nernst equation for the various couples in these biofluids differ.<sup>55</sup> For the redox systems relevant to this work (Table 7), all of which involve two-electron (non-radical) reactions, the Nernst equations are:

$$E = E^{\circ'} - (RT/2F) \ln([\text{RSH}]^2/[\text{RSSR}])$$

and

$$E = E^{\circ'} - (RT/2F) \ln([\text{AA}]/[\text{DHA}])$$

where  $E^{\circ'}/\text{mV}$  (pH = 7.4) has been reported as -264, -250 and +46 for GSSG/GSH, CSSC/CSH and DHA/AA respectively.<sup>56,64</sup> To model such systems in a particular biofluid, it is necessary to estimate the concentrations of the reduced and oxidised species (Table 7). The widely different redox potentials of these couples suggest that they exist in a nonequilibrium steady state, although it is known that they are linked to each other by a continuous transfer of electrons.<sup>55,65</sup>



Table 7 Concentrations and redox potentials for various redox systems\*.

	Blood plasma		Aqueous humour	Lens water
	[X]/(μM)	E/mV	[X]/(μM)	[X]/(μM)
GSH	2.80 ± 0.91 <sup>a</sup>	-137 ± 9 <sup>a</sup>	1.9 ± 0.3 <sup>e</sup>	3280 ± 10 <sup>g</sup>
	3.39 ± 1.04 <sup>b</sup>		5.5 <sup>#f</sup>	
	2.08 ± 0.15 <sup>#c</sup>		0.96 ± 0.14 <sup>#c</sup>	
GSSG	0.14 ± 0.04 <sup>a</sup>		0.006 ± 0.006 <sup>e</sup>	95 ± 25 <sup>g</sup>
	0.27 ± 0.17 <sup>#c</sup>		0.24 ± 0.07 <sup>#c</sup>	
CSH	9.7 ± 3.2 <sup>a</sup>	-80 ± 9 <sup>a</sup>	14.3 <sup>#f</sup>	14.3 <sup>i</sup>
CSSC	40 ± 7 <sup>a</sup>		8 <sup>g</sup>	< 6 <sup>g</sup>
AA	53 ± 12 <sup>d</sup>	+15	10 <sup>3 h</sup>	10 <sup>3 h</sup>
DHA	5 ± 2 <sup>d</sup>		10 <sup>2 h</sup>	

\* GSH, (reduced) glutathione; GSSG, oxidised glutathione (disulfide); CSH, cysteine; CSSC, cystine (disulfide); AA, ascorbic acid; DHA, dehydroascorbic acid. # Patients with cataract. <sup>a</sup> Ref. 56, <sup>b</sup> Ref. 57; <sup>c</sup> Ref. 58; <sup>d</sup> Ref. 59; <sup>e</sup> Ref. 60; <sup>f</sup> Ref. 61; <sup>g</sup> Ref. 62; <sup>h</sup> Ref. 63; <sup>i</sup> (estimated)

**Cytoplasm and blood plasma.** Glutathione and ascorbic acid are considered the most active reducing substances in living tissues.<sup>65</sup> Due to high intracellular GSH concentrations and low [GSSG]/[GHS] ratios, this couple buffers the redox state of cytoplasm with a redox potential of typically -240 to -220 mV.<sup>55,66</sup> In contrast, the redox potentials of CSSC/CSH and DHA/AA are -140 mV<sup>67</sup> and +80 mV<sup>65</sup> respectively.

In blood plasma, the redox potentials of GSSG/GSH and CSSC/CSH differ significantly, implying that the concentrations given in Table 7 refer to a steady state rather than to equilibrium. Plasma redox potentials generally become more oxidising with age but vary in individuals according to oxidative stress-related circumstances.<sup>67</sup> Due to the high CSH concentrations, the CSSC/CSH pool constitutes the major low-molecular-weight thiol/disulfide redox couple in BP, playing a primary role in antioxidant defence and redox signalling between cells and tissues<sup>67</sup> and acting as the predominant redox buffer in plasma.<sup>56</sup> Redox potentials close to the value for this couple have been adopted in our previous modelling of metal ion speciation in plasma (-105 mV,<sup>28</sup> -83 mV<sup>29</sup>). For the present simulation, an intermediate value of -89 mV was selected.

The redox potential of the DHA/AA couple calculated from the concentrations given by Ref. 59 is +15 mV, whereas other workers have reported that DHA is practically absent in the plasma and serum of normal human beings,<sup>68,69</sup> implying a less positive or even negative redox potential for the DHA/AA couple. More recent studies have carefully assessed the analytical uncertainties in the determination of DHA and essentially confirmed the values given in Table 7.<sup>70,71</sup>

**Aqueous humour and lens.** Since AH has a pH of 7.2, calculated  $E^{\circ}$ /mV values change slightly to -252, -238 and +52 for GSSG/GSH, CSSC/CSH and DHA/AA, respectively. Concentrations for GSH and GSSG in AH given by Riley *et al.*<sup>60</sup> correspond to a redox potential of -153 mV, somewhat more negative than for BP. However, GSH concentrations appear to be uncertain as Pandya<sup>72</sup> has reported a value of 32.4 ± 0.9 μM, which is more than

15 times greater than that given by Riley *et al.*<sup>60</sup> The concentrations in Table 7 correspond to a redox potential for the CSSC/CSH couple of  $-97$  mV, slightly more negative than our selected value for BP. Given the likely redox buffering capacity of this couple, due to the high CSH concentration in AH, this value was selected for the present simulation.

Concentrations of AA and DHA in AH have been given as  $1$  mM and  $0.1$  mM respectively,<sup>63</sup> corresponding to a redox potential of  $+21$  mV. There is reasonable agreement about the AA concentration in AH, *e.g.* Pandya<sup>72</sup> has reported a value of  $1180 \pm 33$   $\mu$ M. However, as discussed above for BP, the concentration of  $0.1$  mM DHA (Table 7) is likely to be too high, implying that the actual redox potential for the DHA/AA couple is less positive than  $+21$  mV.

The GSG and GSSG concentrations reported by Dickinson *et al.*<sup>62</sup> (Table 7) suggest a redox potential of  $-223$  mV in “lens water” (the aqueous solution component of the lens, assumed to be 65 % of its total mass<sup>62</sup>).

**Prediction of Cu speciation and metallic Cu(s) precipitation.** JESS is capable of calculating the speciation of Cu(II) and Cu(I) as a function of the prevailing redox potential,  $E_h$ . Metallic copper will become stable when  $E_h \leq E(\text{Cu}^{2+}/\text{Cu(s)})$ , as calculated from the Nernst equation:

$$E = E^\circ(\text{Cu}^{2+}/\text{Cu(s)}) + (RT/2F) \ln[\text{Cu}^{2+}]$$

where  $[\text{Cu}^{2+}]$  is the free  $\text{Cu}^{2+}$  concentration buffered by labile Cu binding to macromolecules<sup>73</sup> such as albumin and other proteins (comprising  $> 95$  % of total Cu).<sup>74</sup> Binding of Cu to small peptides and low-molecular-weight ligands like thioamino acids amounts to about  $0.5$   $\mu$ M in BP, *i.e.* less than 5 %.<sup>74</sup> Values in this range have been found for Cu in serum or plasma ultrafiltrate (eliminating ceruloplasmin, albumin and other proteins expected to bind Cu), but this  $< 30$  kDa fraction was confusingly termed “free Cu”.<sup>75</sup> The actual free (non-complexed) copper (oxidation state not specified) concentration in BP has been estimated to be in the picomolar ( $10^{-12}$  M) range.<sup>74</sup>

The present BP simulation (Table 8) results in a Cu speciation close to those of our previous models.<sup>28,29</sup> Free  $\text{Cu}^+$ , and total  $\text{Cu}^+$  bound to the low-molecular-weight ligands included in the model, are in the concentration ranges given above. In accordance with our earlier simulations,<sup>28,29</sup>  $\text{Cu}^{2+}$  complexes are present only in very small amounts.

The protein content of AH is about 350 times lower than for BP; nevertheless, the fraction of Cu bound to low-molecular-weight ligands is expected to be similar. Assuming the same free  $\text{Cu}^+$  concentration for AH as for BP, the Cu speciation for AH is similar to that in BP but the total  $\text{Cu}^+$  concentration is slightly lower (Table 8).

For ‘lens water’, a significantly lower free  $\text{Cu}^{2+}$  concentration of  $10^{-19}$  M was selected to simulate the strong bonding to proteins and enzymes,<sup>76</sup> which occur in the lens and cornea in high concentrations as part of the oxidative stress defence system. The results (Table 8) indicate a free  $\text{Cu}^+$  concentration lower than in AH but a higher total  $\text{Cu}^+$  concentration. This is a consequence of Cu mobilisation from proteins due to the high ligand (particularly GSH) concentrations (Table 7). It should be noted that due to  $E_h = -223$  mV selected in the present model for ‘lens water’, the free  $\text{Cu}^+$  concentration ( $1.2 \times 10^{-13}$  M) is significantly higher than that of  $\text{Cu}^{2+}$  ( $10^{-19}$  M, see above). In contrast, Rae *et al.*<sup>76</sup> estimated much lower free  $\text{Cu}^+$

concentrations for cytoplasm ( $< 10^{-23}$  M vs.  $< 10^{-18}$  M for  $\text{Cu}^{2+}$ ), which appears to be inconsistent with the strongly reducing conditions maintained in cells.

As shown in Table 8, the present calculations reveal that all three biological fluids are normally under-saturated with respect to Cu(s) under non-pathological conditions, as indicated by the negative logarithmic 'saturation indices'.

In Wilson's disease, however, the synthesis of ceruloplasmin and the excretion of Cu in bile are retarded by a mutation in Wilson ATPase located in hepatocytes. Assuming an increase in labile Cu by a factor of 6 (corresponding to an increase in  $\lg(\text{SI})$  by 0.78) that is typical for Wilson's disease,<sup>75</sup> results in Cu(s) supersaturation and possible deposition in the lens (and cornea, for which similar redox potentials and ligand concentrations are likely<sup>77</sup>) but *not* in blood plasma or aqueous humour. The formation of sunflower cataracts and Kayser-Fleischer rings is therefore directly explicable in terms of the metal-ligand equilibria concerned.

Given the significantly negative redox potential ( $-240$  mV) and high GSH content (*ca.* 5 mM) of cytoplasm,<sup>66</sup> the model further suggests that Cu(s) precipitation in hepatocytes is also likely when Cu excretion is retarded.

The true value of these speciation calculations is that they reveal trends, rather than provide single answers, when different physiological contexts are compared. The species concentrations given in Table 8 should therefore not be taken as absolute values. Rather, they indicate how Cu(I) speciation, and associated properties like Cu(s) supersaturation, change in different biological fluids. Under the conditions simulated in this study, simple equilibrium considerations suggest the predominance of (i) mononuclear complexes since metal concentrations are low and of (ii) binary complexes since the concentrations of CSH and GSH are not simultaneously high; moreover, the only mononuclear species identified in the ternary system ( $\text{Cu}(\text{CS})(\text{GS})\text{H}_4^0$ ) is insignificant at physiological pH.<sup>28</sup> These results are in accord with those obtained from the speciation calculations (Table 8).

Table 8 Copper speciation in various biofluids calculated from the present model at 25 °C and  $I = 0.150$  M

	<b>Biofluids</b>					
	<b>Blood plasma</b> pH= 7.40 pe= -1.50 $E_h = -89$ mV		<b>Aqueous humour</b> pH= 7.20 pe= -1.64 $E_h = -97$ mV		<b>Lens water</b> pH= 7.20 pe= -3.77 $E_h = -223$ mV	
<b>Cu Species*</b>	<b>[Cu]/M</b>	<b>% Cu<sub>total</sub></b>	<b>[Cu]/M</b>	<b>% Cu<sub>total</sub></b>	<b>[Cu]/M</b>	<b>% Cu<sub>total</sub></b>
$\text{Cu}^{\text{I}}(\text{CS})^-$	$1.13 \times 10^{-7}$	65	$1.23 \times 10^{-7}$	83	$1.85 \times 10^{-8}$	2
$\text{Cu}^{\text{I}}(\text{GS})\text{H}^-$	$4.90 \times 10^{-8}$	28	$2.20 \times 10^{-8}$	15	$6.96 \times 10^{-7}$	93
$\text{Cu}^{\text{II}}\text{GlnHis}$	$4.46 \times 10^{-9}$	3	$1.27 \times 10^{-9}$	< 1		
$\text{Cu}^{\text{II}}(\text{His})_2$	$2.44 \times 10^{-9}$	1	$6.72 \times 10^{-10}$	< 1		
$\text{Cu}^{\text{II}}\text{HisThr}$	$1.75 \times 10^{-9}$	1				
$\text{Cu}^{\text{II}}\text{HisTyrH}$	$9.36 \times 10^{-10}$	< 1				
$\text{Cu}_2^{\text{I}}(\text{CS})$			$6.60 \times 10^{-10}$	< 1		
$\text{Cu}^{\text{I}}(\text{GS})_2\text{H}_2^{3-}$					$2.50 \times 10^{-8}$	3
$\text{Cu}^{\text{I}}(\text{GS})^{2-}$					$5.51 \times 10^{-9}$	< 1
$\text{Cu}_2^{\text{I}}(\text{CS})(\text{GS})\text{H}^{2-}$					$1.43 \times 10^{-10}$	< 0.1
$\text{Cu}^+$	$6.68 \times 10^{-12}$	< 0.01	$6.68 \times 10^{-12}$	< 0.01	$1.21 \times 10^{-13}$	< 0.0001
$\text{Cu}_{\text{total}}^{\#}$	$1.74 \times 10^{-7}$	100	$1.47 \times 10^{-7}$	100	$7.45 \times 10^{-7}$	100
lg(SI) of Cu(s)		-1.00		-0.860		-0.471

\* Gln<sup>-</sup> = glutamate, His<sup>-</sup> = histidinate, Thr<sup>-</sup> = threoninate and Tyr<sup>-</sup> = tyrosinate. <sup>#</sup> bound to low-molecular-weight ligands.

## CONCLUSIONS

The protonation constants of three thioamino acids (CSH, PSH and GSH) and the formation constants of their complexes with Cu(I) have been measured in aqueous solution by potentiometric titration using glass electrodes. The characterization of the Cu(I) complexes was particularly difficult because of precipitation of sparingly soluble solids over wide p[H] ranges and the large number of polynuclear and protonated species formed. Precipitation was prevented by the addition of a second thioamino acid, which enabled data to be collected over the whole p[H] range. Detailed numerical analysis yielded the formation constants for the binary systems (involving Cu(I) and only one ligand).

The present results show some similarities to previous studies of these systems but also some significant differences. The most important of these concern the greater number of protonated and polynuclear complexes with different stoichiometries than those previously reported. This is almost certainly due to the much wider p[H] range investigated in this study. The present formation constants are considered to be more realistic for biological applications because they were obtained in a NaCl ionic medium as opposed to previous data measured in different background electrolytes.

A thermodynamic speciation model employing the present constants confirms that Cu(I) is the predominant oxidation state of Cu in blood plasma, aqueous humour, cornea and lens of the human eye. Another important result is the predominance of mononuclear binary complexes of Cu(I) with thioamino acids, consistent with the low Cu(I) concentrations in these biological fluids. When the concentrations of low-molecular-weight Cu complexes are elevated, most commonly as a consequence of Wilson's disease, the precipitation of metallic copper in the eye (as opposed to other tissues) can be reasonably attributed to the mobilisation of Cu into this compartment by the high concentrations of GSH and the corresponding negative redox potential.

## ACKNOWLEDGEMENT

We thank two reviewers for their constructive comments.

## REFERENCES

- 1 G. J. Brewer, *Inorg. Chim. Acta*, 2012, **393**, 135.
- 2 I. Isidoros, I. Delimaris, S. M. Piperakis, *Mol. Biol. Int.*, 2011, DOI: 10.4061/2011/594529.
- 3 M. L. Turski and D. J. Thiele, *J. Biol. Chem.*, 2009, **284**, 717.
- 4 H. Tapiero, D. M. Townsend and K. D. Tew, *Biomed. Pharmacother.*, 2003, **57**, 386.
- 5 D. L. de Romaña, M. Olivares, R. Uauy and M. Araya, *J. Trace Elem. Med. Biol.*, 2011, **25**, 3.
- 6 S. Puig and D. J. Thiele, *Curr. Opin. Chem. Biol.*, 2002, **6**, 171.
- 7 M. Younes and U. Weser, *Biochem. Biophys. Res. Commun.*, 1977, **78**, 1247.
- 8 R. Österberg, in *Biological Roles of Copper*; ed. D. Evered and G. Lawrenson, Ciba Foundation Symposium 79 (New Series, Excerpta Medica: Amsterdam, 1980; pp. 283–292.

- 9 J. J. R. Fausto da Silva and R. J. P. Williams, *The Biological Chemistry of the Elements*, Oxford University Press: Oxford, 2001.
- 10 R. G. Pearson, *Chemical Hardness*; Wiley-VCH: Weinheim, 1997.
- 11 M. P. Brigham, W. H. Stein, S. Moore, *J. Clin. Invest.*, 1960, **39**, 1633.
- 12 S. H. Laurie, D. H. Prime and B. Sarkar, *Can. J. Chem.*, 1979, **57**, 1411.
- 13 L. Hagenfeldt, A. Arvidsson and A. Larsson, *Clin. Chim. Acta*, 1978, **85**, 167.
- 14 R. Österberg, R. Ligaarden and D. Persson, *J. Inorg. Biochem.*, 1979, **10**, 341.
- 15 A. Corazzo, I. Harvey and P. J. Sadler, *Eur. J. Biochem.*, 1996, **236**, 697.
- 16 D. Poger, C. Fillaux, R. Miras, S. Crouzy, P. Delangle, E. Mintz, C. D. Auwer and M. Ferrand, *J. Biol. Inorg. Chem.*, 2008, **13**, 1239.
- 17 P. Crea, A. De Robertis, C. De Stefano, D. Milea and S. Sammartano, *J. Chem. Eng. Data*, 2007, **52**, 1028.
- 18 J. M. Walshe, *Am. J. Med.*, 1956, **21**, 487.
- 19 M. M. Jones, *Crit. Rev. Toxicol.*, 1991, **21**, 209.
- 20 I. A. Jaffe, *Arth. Rheum.*, 1970, **13**, 436.
- 21 M. Micheloni, P. M. May and D. R. Williams, *J. Inorg. Nucl. Chem.*, 1978, **40**, 1209.
- 22 N. N. Greenwood and A. Earnshaw, *Chemistry of the Elements*; Elsevier, 2<sup>nd</sup> edn, 1997.
- 23 G. Berthon, *Pure & Appl. Chem.*, 1995, **67**, 1117.
- 24 W. Stricks and I. M. Kolthoff, *J. Am. Chem. Soc.*, 1951, **73**, 1723.
- 25 S. P. Mezyk and D. A. Armstrong, *Can. J. Chem.*, 1989, **67**, 736.
- 26 M. J. Walsh and B. A. Ahner, *J. Inorg. Biochem.*, 2013, **128**, 112.
- 27 G. T. Hefter, P. M. May and P. Sipos, *J. Chem. Soc., Chem. Commun.*, 1993, 1704.
- 28 L.-C. Tran-Ho, P. M. May and G. T. Hefter, *J. Inorg. Biochem.*, 1997, **68**, 225.
- 29 P. M. May, *Appl. Geochem.*, 2015, **55**, 3.
- 30 F. C. J. Rossotti and H. Rossotti, *J. Chem. Educ.*, 1965, **42**, 375.
- 31 L.-C. Tran-Ho, Honours Thesis, Murdoch University, Western Australia, 1991.
- 32 L.-C. Koenigsberger, E. Königsberger, P. M. May and G. T. Hefter, *J. Inorg. Biochem.*, 2000, **78**, 175.
- 33 J. Mendham, R. C. Denney, J. D. Barnes, M. J. K. Thomas, *Vogel's Text-Book of Quantitative Inorganic Analysis*, 6th edition, Pearson Education Limited, Harlow, 2000.
- 34 P. M. May, K. Murray and D. R. Williams, *Talanta*, 1988, **35**, 825.
- 35 P. M. May and K. Murray, *Talanta*, 1988, **35**, 927.
- 36 P. M. May and K. Murray, *Talanta*, 1988, **35**, 933.
- 37 H. Rossotti, *The Study of Ionic Equilibria*, Longman: London, 1978.
- 38 A. Tromans, G. Hefter, P. M. May, *Aust. J. Chem.*, 2005, **58**, 213.
- 39 V. K. Sharma, F. Casteran, F. J. Millero, C. De Stefano, *J. Solution Chem.*, 2002, **31**, 783.
- 40 Y. Bizri, M. Cromer-Morin and J.-P. Scharff, *J. Chem. Research (S)*, 1982, 192.
- 41 M. Jawaid and F. Ingman, *Talanta*, 1981, **28**, 137.
- 42 G. R. Lenz and A. E. Martell, *Biochemistry*, 1964, **3**, 745.
- 43 A. P. Arnold and A. J. Canty, *Can. J. Chem.*, 1983, **61**, 1428.
- 44 W. Stricks and I. M. Kolthoff, *J. Am. Chem. Soc.*, 1953, **75**, 5673.
- 45 V. Vortisch, P. Kroneck and P. Hemmerich, *J. Am. Chem. Soc.*, 1976, **98**, 2821.
- 46 G. A. Bagiyani, I. K. Koroleva and N. V. Soroka, *Russ. J. Inorg. Chem.*, 1978, **23**, 1337.
- 47 L. G. Sillén and A. E. Martell, *Stability Constants of Metal-Ion Complexes*, Supplement No. 1, Special Publication No. 25, London: The Chemical Society: London, 1971.

- 48 P. Sipos, Murdoch University, Australia. Personal communication.
- 49 B. Harman, I. Sívágó, *Inorg. Chim. Acta*, 1983, **80**, 75.
- 50 E. Aydin, T. Cumurcu, F. Özüğurlu, H. Özyurt, S. Sahinoglu, D. Mendil and E. Hasdemir, *Biol. Trace Elem. Res.*, 2005, **108**, 33.
- 51 J. C. Suvarna, *J. Postgrad. Med.*, 2008, **54**, 238.
- 52 J. E. Cairns, H. P. Williams and J. M. Walshe, *Brit. Med. J.*, 1969, **3**, 95.
- 53 F. Sharifipour, E. Idani, M. Zamani, T. Helmi and B. Cheraghian, *J. Ophthalmic. Vis. Res.*, 2013, **8**, 119.
- 54 P. M. May, *J. Chem. Soc., Chem. Commun.*, 2000, 1265.
- 55 M. Kemp, Y.-M. Go and D. P. Jones, *Free Radical Biol. Med.*, 2008, **44**, 921.
- 56 D. P. Jones, J. L. Carlson, V. C. Mody Jr., J. Cai, M. J. Lynn and P. Sternberg Jr., *Free Radical Biol. Med.*, 2000, **28**, 625.
- 57 F. Michelet, R. Gueguen, P. Leroy, M. Wellman, A. Nicolas and G. Siest, *Clin. Chem.*, 1995, **41**, 1509.
- 58 E. Stahl, R. Buhl, O. Schnaudigel, G. Steinkamp, U. Fries, H. Gumbel and C. Ohrloff, *Ophthalmologie*, 1996, **93**, 54.
- 59 S. S. Dubey, G. Roy Palodhi and A. K. Jain, *Ind. J. Physiol. Pharmac.*, 1987, **31**, 279.
- 60 N. V. Riley, R. F. Meyer and E. M. Yates, *Invest. Ophthalmol. Vis. Sci.*, 1980, **19**, 94.
- 61 S. P. Richer and R. C. Rose, *Vision Res.*, 1998, **38**, 2881.
- 62 J. C. Dickinson, D. G. Durham and P. B. Hamilton, *Invest. Opth.*, 1968, **7**, 551.
- 63 A. Umapathy, P. Donaldson and J. Lim, *BioMed Res. Int.*, 2013, DOI: 10.1155/2013/207250.
- 64 E. G. Ball, *J. Biol. Chem.*, 1937, **118**, 210.
- 65 B. S. Winkler, S. M. Orselli and T. S. Rex, *Free Radic. Biol. Med.*, 1994, **17**, 333.
- 66 F. Q. Schafer and G. R. Buettner, *Free Radic. Biol. Med.*, 2001, **30**, 1191.
- 67 Y.-M. Go and D. P. Jones, *Biochim. Biophys. Acta*, 2008, **1780**, 1273.
- 68 I. B. Chatterjee and A. Banerjee, *Anal. Biochem.*, 1979, **98**, 368.
- 69 K. R. Dhariwal, W. O. Hartzell and M. Levine, *Am. J. Clin. Nutr.*, 1991, **54**, 712.
- 70 I. Koshiishi and T. Imanari, *Anal. Chem.*, 1997, **69**, 216.
- 71 I. Koshiishi, Y. Mamura, J. Liu and T. Imanari, *Biochim. Biophys. Acta*, 1998, **1425**, 209.
- 72 A. V. Pandya, *World Journal of Pharmaceutical Research*, 2014, **3**, 1112.
- 73 P. M. May, P. W. Linder and D. R. Williams, *J. Chem. Soc. Dalton Trans.*, 1977, 588.
- 74 M. C. Linder, *Mutat. Res.*, 2001, **475**, 141.
- 75 G. A. McMillin, J. J. Travis and J. W. Hunt, *Am. J. Clin. Pathol.*, 2009, **131**, 160.
- 76 T. D. Rae, P. J. Schmidt, R. A. Pufahl, V. C. Culotta and T. V. O'Halloran; *Science*, 1999, **284**, 805.
- 77 A. Shoham, M. Hadziahmetovic, J. L. Dunaief, M. B. Mydlarski and H. M. Schipper, *Free Radical Biol. Med.*, 2008, **45**, 1047.